A GEOMETRIC APPROACH TO INVARIANT SETS FOR DYNAMICAL SYSTEMS

DAVID MEDINA, PABLO PADILLA

Abstract. In this article, we present a geometric framework to study invariant sets of dynamical systems associated with differential equations. This framework is based on properties of invariant sets for an area functional. We obtain existence results for heteroclinic and periodic orbits. We also implement this approach numerically by means of the steepest descent method.

1. Introduction

In this work, we consider the area generated by a curve under the action of the flow defined by an autonomous differential equation. To fix ideas we work in $\mathbb{R}^2$ although the method is completely general.

This approach has been considered by Smith [9] as well as by Li and Muldowney [3, 4, 5, 6, 7]. The first author establishes bounds on the Hausdorff dimension of ω-limit sets. The last two authors extend the Bendixson's criterion for nonexistence of periodic solutions and give stability results for some periodic orbits based on area functionals.

The main goal of this paper is to obtain invariant sets considering a functional that describes the area that generates a curve under a flow and observing that the functional vanishes on invariant curves and, conversely, whenever its infimum is achieved at a curve of finite length, then this curve is invariant (see Theorem 2.1). This variational principle is used in order to obtain a numerical implementation that will give us an approximation to this curve by employing the steepest descent method. This implementation is done in the cases of heteroclinic orbits and limit cycles.

---

2. The area functional and invariant sets

Given a dynamical system defined on a set X, its evolution is described by a monoparametric family of operators $\{S(t)\}_{t \geq 0}$, that maps X into itself and possesses the standard semigroup properties:

$$S(t+s) = S(t) \cdot S(s), \quad \forall s, t \geq 0,$$
$$S(0) = I.$$

The basic property of this family is that $S(t)$ is a continuous operator from X to X.

A set $Y \subset X$ is *positively invariant* for $S(t)$ if

$$S(t)Y \subset Y, \quad \forall t > 0, \tag{2.1}$$

and *negatively invariant* if

$$S(t)Y \supset Y, \quad \forall t > 0. \tag{2.2}$$

When the set is both positively and negatively invariant we say that it is an invariant set. Thus, a set $Y \subset X$ is an invariant set for the semigroup $\{S(t)\}_{t \geq 0}$ if

$$S(t)Y = Y, \quad \forall t \geq 0. \tag{2.3}$$

The simplest examples of invariant sets are equilibrium points, heteroclinic orbits and limit cycles.

A *heteroclinic orbit* is a solution in phase space that joins two different equilibrium points. One of them the ω-limit set of this orbit and the other its α-limit set.

A *stable limit cycle* is a closed trajectory in phase space such that any trajectory nearby spirals into it when t increases.

To describe the characterization of invariant sets through an area functional, let us consider the case where $S(t)$ is generated by the differential equation

$$\dot{x} = f(x), \tag{2.4}$$

where f is a vector field in $\mathbb{R}^2$.

Thus, for a curve $\gamma(s)$, where γ is assumed to be parameterized by arc length $\gamma : [s_0, s_1] \to \mathbb{R}^2$, $S(t)\gamma(s)$, for some fixed $t \in [0, T]$ represents the *displaced curve* under the flow generated by S at time t. Analogously, if we consider $S(t)\gamma(s)$ for all $t \in [0, T]$ and all $s \in [s_0, s_1]$ we obtain a strip on the phase plane, as shown in figure 1.

Assume that x_0 and x_1 are fixed points of (2.4) (i.e. $f(x_0) = 0$, $f(x_1) = 0$) and $\gamma(s)$ is a continuous curve that joins these points, with $\gamma(s_0) = x_0$ and $\gamma(s_1) = x_1$. Let Γ be the set of these curves. Thus, "an element of area", is given by $|f(\gamma(s)) \times \dot{\gamma}(s)|$, as shown in figure 2.

Therefore the area, $A_t(\gamma(s))$, is given by:

$$A_t(\gamma(s)) = \left(\int_{s_0}^{s_1} |f(\gamma(s)) \times \dot{\gamma}(s)| \, ds \right) + o(t). \tag{2.5}$$

It is clear that if the curve is invariant then $A_t(\gamma(s)) = 0$. The converse is also true under appropriate assumptions.

Since the functional is bounded from below (clearly $A_t \geq 0$), then a natural way to study invariant sets is through the minimization of A_t.
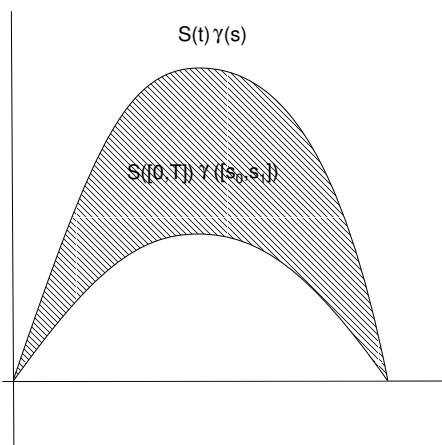
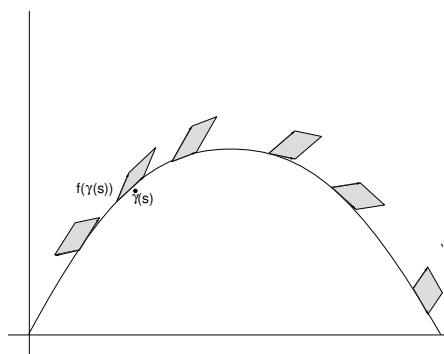FIGURE 1. Strip generated by a curve under a flow.

FIGURE 2. Differential element for the area functional.

Let be $A^*(\gamma) = \int_{s_0}^{s_1} |\dot{\gamma} \times f| \, ds$, l fixed and $\Gamma_l = \{\gamma \in \Gamma | \text{length}(\gamma) \leq l\}$. If the infimum of the area functional is zero in Γ and equal to the infimum in Γ_l then this infimum will be an invariant curve, as established in the following theorem.

Theorem 2.1. *If there is an l such that $\inf_\Gamma A = \inf_{\Gamma_l} A^*$ and $\inf_\Gamma A^* = 0$, then $\inf_\Gamma A^*$ is attained in some γ^* that is invariant under the flow generated by* (2.4).

Proof. Without loss of generality, we can work in Γ_l. (Γ_l is bounded and equicontinuous by hypothesis). Let γ_n be a minimizing sequence in Γ_l. By Arzela - Ascoli's theorem there is a subsequence γ_{n_j} such that $\gamma_{n_j} \xrightarrow{unif} \gamma^*$. By Fatou's lemma

$$0 \leq \int_{s_0}^{s_1} |\dot{\gamma}^* \times f(\gamma^*)| = \int_{s_0}^{s_1} \liminf |\dot{\gamma}_{n_j} \times f(\gamma_{n_j})| \leq \lim \int_{s_0}^{s_1} |\dot{\gamma}_{n_j} \times f(\gamma_{n_j})| \to 0.$$

Therefore, $|\dot{\gamma}^* \times f(\gamma^*)| = 0$, $\forall$ s $\in [s_0, s_1]$. This implies that $\dot{\gamma}^*$ is parallel to $f(\gamma^*)$ and so γ^* is invariant for the flow generated by (2.4).   □

Remark 2.2. In general, the equality $\inf_\Gamma A = \inf_{\Gamma_l} A^*$ does not hold, since $\Gamma_l \subset \Gamma$. This fact only implies that $\inf_\Gamma A \leq \inf_{\Gamma_l} A^*$.

Remark 2.3. Consider the phase portrait and in particular the orbits shown in figure 3. In this case, any curve that joins x_0 and x_1 with finite length generates a region of strictly positive area. The infimum is not attained in the class of curves with finite length, and therefore can not be an invariant curve. Similar examples can be constructed by considering the irrational flow on the torus.
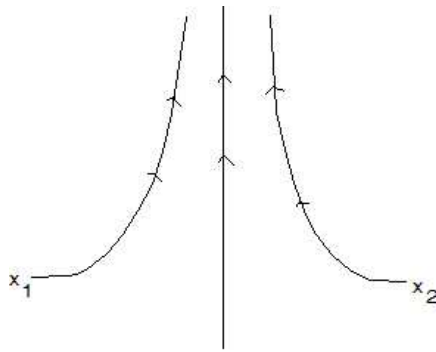

FIGURE 3. Phase portrait of a nonrectifiable curve wich is not invariant.

3. NUMERICAL IMPLEMENTATION

Theorem 2.1 guarantees that the infimum of the area functional is attained at some curve. However, we do not have an analytic or approximate expression. In what follows, we show that the variational principle can be used numerically to approximate this curve. To obtain this approximation, we use the functional

$$\tilde{A}(\gamma(s)) = \int_{s_0}^{s_1} |f(\gamma(s)) \times \dot{\gamma}(s)|^2 \, ds, \tag{3.1}$$

because it is convenient from the numerical point of view, but clearly if $\tilde{A}$ vanishes at a curve, so does A_t.

Consider as an application the physical pendulum and corresponding separatrices; i. e., the two heteroclinic orbits that join $(-\pi, 0)$ with $(\pi, 0)$. The equation reads

$$\ddot{x} = -\sin x \tag{3.2}$$

or equivalently,

$$(\dot{x}, \dot{y}) = (y, -\sin x). \tag{3.3}$$

Note that (3.2) and (3.3) constitute a conservative system (see [1]), in which the total energy

$$E = \frac{1}{2}\dot{x}^2 + U(x),$$

where
$$U(x) = \int_0^x \sin \eta \, d\eta = 1 - \cos x,$$
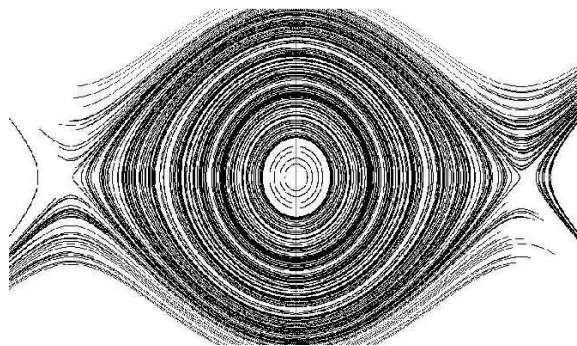is conserved. Its phase portrait is shown in figure 4.

FIGURE 4. Phase portrait of system (3.3).

The separatrix lies on the level curve $E = 2$ and is given by
$$\frac{1}{2}y^2 - \cos x - 1 = 0. \tag{3.4}$$
Therefore, the upper part of (3.4) is parameterized by
$$(s, \sqrt{2\cos s + 2}), \ -\pi \le s \le \pi. \tag{3.5}$$

Now, suppose that $(s, v(s))$ is an approximation to (3.5), which satisfies $v(\pm\pi) = 0$. Under this assumption, we calculate the area functional $\tilde{A}$ given by (3.1) generated by the flow (3.3). A straightforward calculation gives that $\tilde{A}(\gamma(s))$ for $\gamma(s) = (s, v(s))$ is
$$\tilde{A}(\gamma(s)) = \int_{-\pi}^{\pi} (\sin s + v(s)v'(s))^2 ds. \tag{3.6}$$

Now, we take
$$v(s) = -(s + \pi)(s - \pi)\sum_{i=0}^{n} a_i s^i, \tag{3.7}$$
which clearly satisfies $v(\pm\pi) = 0$.

Note that in (3.6), the a_i's values mentioned in (3.7) are taken as *variables*. For some choice of these values, we obtain a parameterized curve. Thus, we want to find the choice of these coefficients such that (3.7) be the *best approximation* to the invariant curve.

The steepest descent method (or gradient method) is one of the simplest and the most useful minimization methods for unconstrained optimization, which is based in successive approximations and it "follows" minus gradient of the function, because it represents the direction in which the function decreases most quickly. The iteration is:
$$x_{i+1} = x_i - \epsilon \nabla \tilde{A}(x_i), \tag{3.8}$$
where x_i is the i-th iteration , ϵ is a small value and $\nabla \tilde{A}(x_i)$ represents the gradient of the area functional evaluated at the i-th iteration.

To determine the convergence of (3.8), we use the following criterion:

(1) Select a parameter $\delta > 0$.
(2) Calculate $\mathbf{c} = \nabla f(x_i)$. If $\|\mathbf{c}\| < \delta$ then x_i is the sought approximation, else repeat.

For a more detailed description about this method, see for example [2, 8].

Now, we choose $n = 2$ in (3.7), due to the symmetry of the separatrix with respect to the y-axis, and consider the *initial guess* $(2.03, 0, -0.27)$, $\epsilon = 0.000009$, and $\delta = 0.0011$. These values were chosen because they represent a good approximation to the exact values for the Taylor expansion of (3.5). Observe that the corresponding value of the norm in the 2000-th iteration is 0.001055164525. This fact shows convergence of this method according to the criterion previously established. These results are shown in figures 5 to 8. The invariant curve is below the approximating curves. Apparent changes is size are due to scaling.
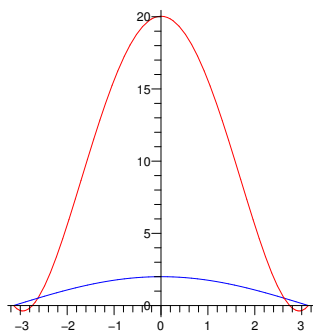
FIGURE 5. Initial curve versus invariant curve.
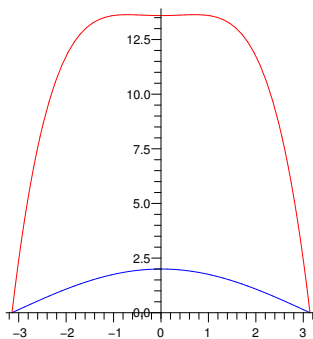
FIGURE 6. First iteration versus invariant curve.

On other hand, if we consider (clearly does not satisfy $v(\pm\pi) = 0$)
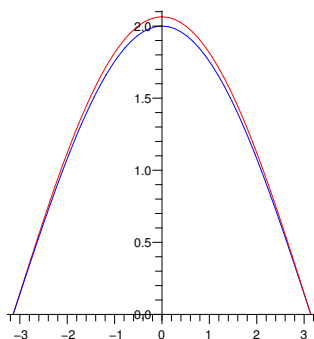
$$v(s) = \sum_{k=0}^{n} a_k s^k \qquad (3.9)$$

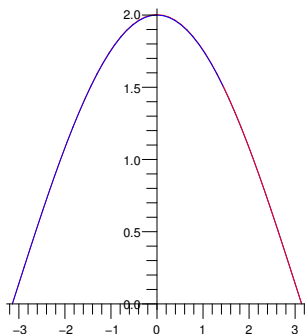FIGURE 7. 500-th iteration versus invariant curve.

FIGURE 8. 1000-th iteration versus invariant curve.

instead of (3.7), we choose $n = 11$ (a truncated Taylor series) and the initial guess:

$$(2.03, 0, -0.27, 0, 6 \times 10^{-3}, 0, -5 \times 10^{-5}, 0, 1.95 \times 10^{-7}, 0, -6 \times 10^{-10}) \quad (3.10)$$

We fix $\epsilon = 3 \times 10^{-10}$. A graphical representation of the initial curve is shown in figure 9. Then we obtain the curve after 10 iterations and compare it with the corresponding invariant curve (see figure 10).

When considering (3.9)-(3.10), the value of the gradient of the area functional after 10 iterations is 2356.113011. This fact shows that it is not a convenient choice.

4. APPLICATION TO LIMIT CYCLES

In this section we shall see how to extend the previous ideas to the study of limit cycles. Since these sets are closed curves, we use truncated Fourier series instead of polynomials in order to approximate them. Let us consider:

$$\dot{x_1} = -x_2 + x_1(x_1^2 + x_2^2 - 1) \quad (4.1)$$

$$\dot{x_2} = x_1 + x_2(x_1^2 + x_2^2 - 1). \quad (4.2)$$
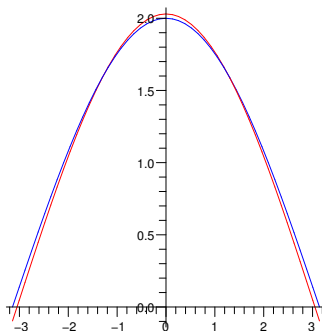
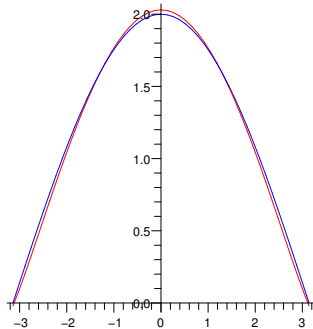FIGURE 9. Initial curve versus invariant curve.

FIGURE 10. Graph of 10-th iteration versus invariant curve.

By using polar coordinates, we see that $x_1^2 + x_2^2 = 1$ is a stable limit cycle (see figure 11).
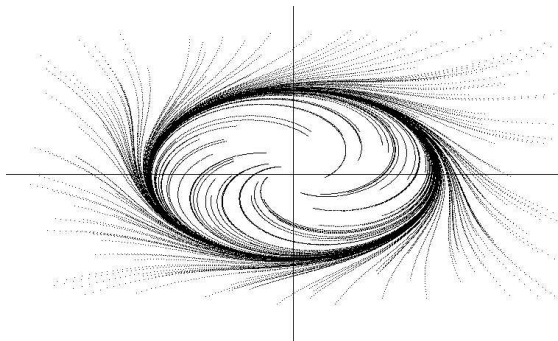

FIGURE 11. Phase portrait of (4.1)-(4.2).

To characterize this limit cycle by minimization of the functional $\tilde{A}$ given by (3.1), we use the usual parametrization

$$\gamma(s) = (\cos s, \sin s), \ 0 \leq s \leq 2\pi. \tag{4.3}$$

Assume that

$$u(s) = \sum_{k=0}^{2} a_k \cos ks + \sum_{k=1}^{2} b_k \sin ks, \tag{4.4}$$

$$v(s) = \sum_{k=0}^{2} a'_k \cos ks + \sum_{k=1}^{2} b'_k \sin ks, \tag{4.5}$$

is a finite approximation to (4.3). Therefore,

$$\tilde{A}(\gamma(s)) = \int_0^{2\pi} ((-v + u(1 - u^2 - v^2))v' - (u + v(1 - u^2 - v^2))u')^2 \, ds. \tag{4.6}$$

We choose $\epsilon = 0.005$ and $\delta = 0.0006$ in order to apply steepest descent to this functional. The corresponding initial guess is

$$(0, 1.3, 0.1, 0.1, 0.1, 0.1, 0.1, 0.01, 1.3, 0.1). \tag{4.7}$$

Since $|\nabla \tilde{A}(x_{110})| < 0.0006$, we obtain convergence as shown in figures 12-15.
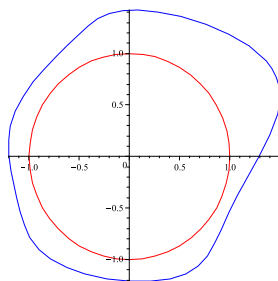

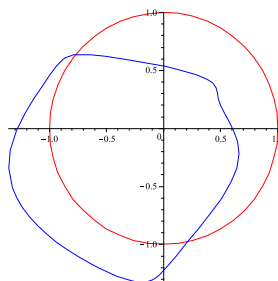FIGURE 12. Initial guess versus stable limit cycle of (4.1)-(4.2).

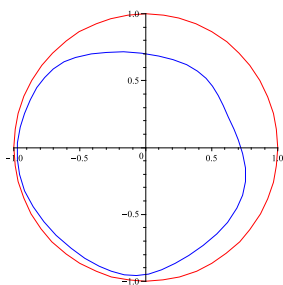FIGURE 13. First iteration versus stable limit cycle.

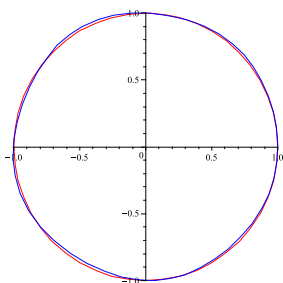FIGURE 14. 10-th iteration versus stable limit cycle.

FIGURE 15. 111-th iteration versus stable limit cycle.

On other hand, if we consider

$$\dot{x_1} = -x_2 + x_1(x_1^2 + x_2^2 - 1)^2 \tag{4.8}$$

$$\dot{x_2} = x_1 + x_2(x_1^2 + x_2^2 - 1)^2 \tag{4.9}$$

instead of (4.1)-(4.2), then $x_1^2 + x_2^2 = 1$ is an unstable limit cycle (see figure 16).
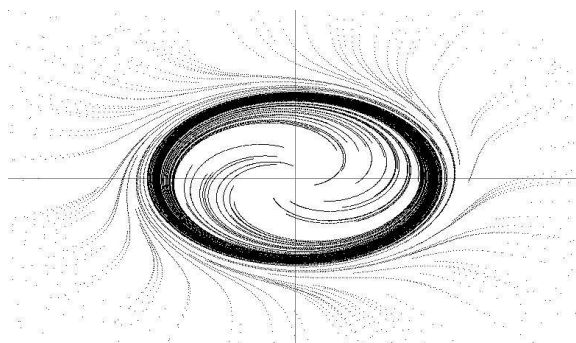

FIGURE 16. Phase portrait of (4.8)-(4.9).

As before, we use (4.4)-(4.5), $\epsilon = 0.005$, $\delta = 0.0055$ and the initial guess:

$$(0, 1.2, 0.1, 0.1, 0.1, 0.1, 0.1, 0.01, 1.1, 0.1).$$

Since $|\nabla \tilde{A}(x_{400})| < 0.0055$, we obtain convergence as shown in figures 17–20.
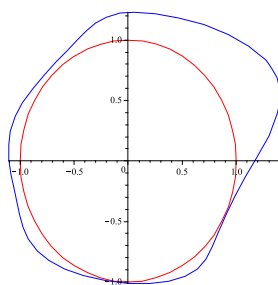
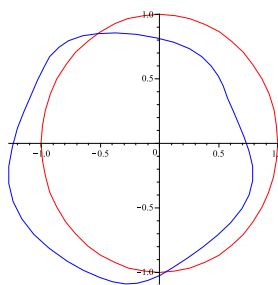FIGURE 17. Initial guess versus unstable limit cycle of (4.8)-(4.9).

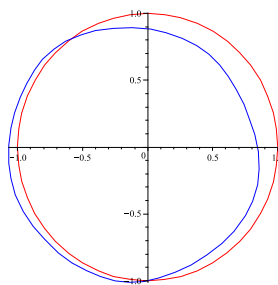FIGURE 18. First iteration versus unstable limit cycle.

FIGURE 19. 10-th iteration versus unstable limit cycle.

REFERENCES

[1] Arnold V. I., *Mathematical Methods of Classical Mechanics*, Graduate Text in Mathematics, Springer - Verlag, 1989.

[2] Bonnans J. F., et. al. *Numerical Optimization: Theoretical and Practical Aspects*, Universitext, Springer-Verlag, 2006.

[3] Li Yi M. and Muldowney James S., *On R. A. Smith's autonomus convergence theorem*, Rocky Mountain Journal of Mathematics, volume 25, number 1, 365–381, 1995.

[4] Li Yi M. and Muldowney James S., *On Bendixson's Criterion*, Journal of Differential Equations 106, 27–39, 1993.

[5] Li Yi M. and Muldowney James S., *Evolution of surface functionals and differential equations*, Ordinary and Delay Differential Equations, Longman Scientific and Technical, 144–148, 1992.
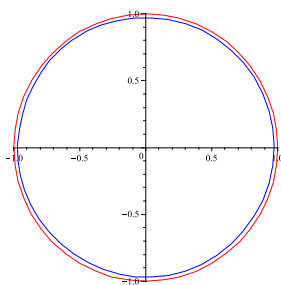
FIGURE 20. 110-th iteration versus unstable limit cycle.

[6] Li Yi M. and Muldowney James S., *Lower bounds for the Haussdorff dimension of attractors*, Journal of Dynamics and Differential Equations 7, 455–467, 1995.

[7] Li Yi M. and Muldowney James S., *Dynamics of differential equations on invariant manifolds*, Journal of Differential Equations 168, 295–320, 2000.

[8] Peressini A. L., et. al., *The Mathematics of Nonlinear Programming*, Undergraduate Text in Mathematics, Springer-Verlag, 1988.

[9] Smith R. A., *Some Applications of Hausdorff dimension inequalities for ordinary differential equations*, Proy. Roy. Soc. Edinburg Sect. A 104, 235–259, 1986.

DAVID MEDINA
INSTITUTO TECNOLÓGICO SUPERIOR DE PEROTE, CARRETERA PEROTE-MÉXICO KM. 2.5, CENTRO, PEROTE, VERACRUZ, C. P. 91270, MÉXICO
E-mail address: `medina@math.unam.mx`

PABLO PADILLA
DEPARTAMENTO DE MATEMÁTICAS Y MECÁNICA, IIMAS-UNAM, APARTADO POSTAL 20-726, C. P. 01000 MÉXICO, MÉXICO
E-mail address: `pablo@mym.iimas.unam.mx`